Termination of hollow core nanopipes in GaN by an AlN interlayer

O. Contreras, F. Ruiz-Zepeda, M. Avalos-Borja, A. Dadgar, A. Krost

www.elsevier.com/locate/jcrysgro

PII: S0022-0248(16)30525-5
DOI: http://dx.doi.org/10.1016/j.jcrysgro.2016.09.027
Reference: CRYS23585

To appear in: *Journal of Crystal Growth*

Received date: 12 March 2016
Revised date: 27 July 2016
Accepted date: 13 September 2016

Cite this article as: O. Contreras, F. Ruiz-Zepeda, M. Avalos-Borja, A. Dadgar and A. Krost, Termination of hollow core nanopipes in GaN by an AlN interlayer, *Journal of Crystal Growth* http://dx.doi.org/10.1016/j.jcrysgro.2016.09.027

Termination of hollow core nanopipes in GaN by an AlN interlayer

O. Contreras[1*], F. Ruiz-Zepeda[2*], M. Avalos-Borja[3,1], A. Dadgar[4], A. Krost[4]

[1]Centro de Nanociencias y Nanotecnología, Universidad Nacional Autónoma de México, Apdo. Postal 356, Ensenada, Baja California C.P. 22800, Mexico

[2]Laboratory for Materials Chemistry, National Institute of Chemistry, Hajdrihova 19, SI-1000 Ljubljana, Slovenia

[3]Instituto Potosino de Investigación Científica y Tecnológica, División de Materiales Avanzados, San Luis Potosí, SLP, Mexico

[4]Otto-von-Guericke-Universität Magdeburg, FNW-IEP, Universitätsplatz 2, 39106 Magdeburg, Germany

edel@cnyn.unam.mx

Francisco.ruizzepeda@ki.si

[*]Author to whom correspondence should be addressed:

Abstract

Nanopipes associated to screw dislocations are studied by transmission electron microscopy in Si-doped GaN films grown on silicon substrates. The observations revealed that dislocations had an empty core and that an AlN interlayer is suited to block their propagation. The termination mechanism is discussed in terms of strain and kinetic growth factors, which may affect the creation and propagation of nanopipes. According to the observations, it is proposed that either step pinning or lateral overgrowth occurring at the proximity of the defect assists in capping the nanopipe.

Keywords

A1. Nanostructures; A1. TEM; A1. Nanopipes; A3. Metal Organic Vapor Phase Epitaxy; B1. GaN; B2. Semiconducting III-V materials

1. Introduction

GaN growth on silicon substrates has been successfully implemented in products as devices for blue-light emitting diodes (LEDs), laser diodes (LDs) and additionally, field effect transistors (FETs) [1-7]. From the industrial-cost point of view, it is more convenient to integrate the crystal growth of GaN to the already well stablished silicon technology in electronic circuit systems, which are based on large silicon wafers, since it offers lower prices compared to its substrate competitors SiC and sapphire [8-10]. Currently, there are several challenges to grow defect-free GaN bulk crystals, although efforts to implement homoepitaxial growth are being made [11-15], foreign substrates are the next option. However, between hexagonal GaN and the most common used substrates, SiC and sapphire, there is a large lattice mismatch and a considerable difference between the thermal expansion coefficients, causing a high density of structural threading defects in the GaN film during growth. Depending on the growth conditions, these defects can be, dislocations of edge-type: **a** dislocations with Burgers vectors $\mathbf{b} = 1/3\langle 1\bar{1}20\rangle$, screw-type: **c** dislocations with Burgers vectors $\mathbf{b} = \langle 0001\rangle$, or mixed-type: **c**+**a** dislocations with Burgers vectors $\mathbf{b} = 1/3\langle 11\bar{2}3\rangle$, where the magnitudes *a*, *c* are the unit cell parameters. Other type of defects can also populate the film, such as stacking faults, inversion domains or nanopipes [16]. It has been showed previously, that dislocations are unfavorable to the quality of GaN layers when crossing the semiconductor device active regions, acting as non-recombination centers, short-circuits or leading to low breakdown voltages in high voltages devices. Screw dislocations, in general, have a more harmful effect in gate leakage than edge or mixed dislocations [17]. Specially, open core screw-type dislocations have been referred as responsible for

leakage current in GaN based LEDs [18]. Recently, a study demonstrated that open core screw-type dislocations have a particularly detrimental effect on LEDs performance despite its small fraction of the total density of dislocations [19], and that they exhibited a more significant leakage current than pure screw-type dislocations [20]. The development of methods to reduce or annihilate dislocations [21-25], and the study of models to predict how dislocations will behave under certain conditions [26, 27], are of great importance when engineering film growth. Transmission electron microscopy (TEM) analysis can provide insight to the epilayers microstructure and has been the tool of choice to study such defects in GaN films [28-30].

Nanopipes are defined as hollow tubes with nanometer scale diameters and $\{1\bar{1}00\}$ faceted sides. Some of them can be associated with open core screw-type dislocations with larger Burgers vectors, $|\mathbf{b}|=\pm n\mathit{c}$ (with n>1) [30, 31]. Accidental growth mechanisms, growth mode or doping (Si, O, Mg) can influence the creation of nanopipes [32, 33]. Impurity segregation such as oxygen has been shown to influence nanopipes growth, which are expected to originate at the surface of pits [33, 34]. By getting insights of their characteristics we can find better methods to reduce this type of defects in thin films, since only an open surface or a grain boundary can stop their propagation. In this study, we examine the presence of nanopipes in Si doped GaN films grown on Si(111) using transmission and scanning transmission electron microscopy (TEM and STEM, respectively). By using energy dispersive x-ray spectroscopy (EDX) profiles and high angle annular dark field imaging (HAADF) it is shown that the nanopipes studied here have a hollow core. These hollow nanopipes are fully constricted and in some cases do not open at the GaN surface like V defects [33, 35, 36]. Instead, nanopipes terminate at

AlN interlayers introduced in GaN films; an implemented growth method to reduce stress in the GaN films grown on Si [37, 38]. Models explaining the associated dislocation behavior and termination mechanisms for these type of nanopipes are proposed.

2. Experimental methods

Microstructural studies were carried out on two sets of specimens with different interlayer design. The samples were grown by metal organic vapor phase epitaxy (MOVPE). The first type of specimen was a single Si-doped GaN layer ~1 μm thick, grown at 1050 °C on a Si(111) substrate with a 25 nm AlN seed layer deposited at 720 °C. The second type of specimen consisted of a stack of three 430 nm Si-doped GaN layers grown under the same growth conditions as the first sample but separated by two 15 nm AlN layers grown at 720 °C (Figure S1). Prior to the growth process, the silicon substrates were chemically etched in order to remove the oxide layer and leave a hydrogen-terminated surface [39]. Characterization of the film/substrate interface and of the AlN buffer layer, has been previously reported [37, 40, 41]. Cross-section and plan view TEM specimens were prepared by wedge polishing followed by Ar+ ion-milling. TEM observations were performed in a JEM 4000EX JEOL instrument operating at an acceleration voltage of 400 kV. STEM HAADF imaging and EDX measurements were performed in a FEI TECNAI-F30 operating at 300 kV.

3. Results and discussion

To reveal screw and edge type dislocations, cross sectional TEM images of the single GaN layer were taken under $\mathbf{g}=[0001]$ and $\mathbf{g}=[1\bar{1}00]$ diffraction conditions (Figure S2).

A straight defect parallel to the [0001] growth direction associated to screw type is shown in Fig. 1(a) with **g**=[0001] imaging conditions [42]. The defect apparently starts to grow from the AlN nucleation layer and shows a constant width through the entire epilayer. The tubular shape of this defect is a distinguishable characteristic of a nanopipe [43].

Only nanopipes associated to screw-type dislocations were found. The size of the nanopipes ranged from 2 to 10 nm, being around ~5-6 nm the most frequently observed size. In Fig. 1(b) a schematic representation of a screw type dislocation with full core and open core is depicted and in Fig. 1(c) a high resolution TEM plan view bright field image of the top end of a nanopipe at the surface of the single GaN film is shown. The diameter of the nanopipe is approximately 6.5 nm showing $\{1\bar{1}00\}$ facets corresponding to the hexagonal prism planes, where the surrounding crystalline material abruptly ends. The contrast observed in the core is characteristic of an amorphous phase which may be have been introduced as contaminant during TEM sample preparation [44, 45]. Previous atomic force microscopy (AFM) studies [23] revealed the presence of uniform holes associated to nanopipes emerging out at the top surface of the single GaN layer which were not filled with material at the top (Figure S3).

In the three stacked GaN layered structure, nanopipes were observed to terminate at the first AlN interlayer. A HRTEM image of a nanopipe ending at the AlN interlayer is shown in Fig. 2. The nanopipe does not end sharply at the AlN/GaN interface, but penetrates a few monolayers into the AlN interlayer. The cap of the nanopipe is not flat, meaning that the nanopipe does not close quickly during AlN growth [46]. In general, the nanopipes showed a full columnar constricted shape and all of them terminated at the first

AlN interlayer. In our observations we did not find more nanopipes in subsequent GaN layers (Figure S4). Top surface images of these structures also revealed no holes on the surface [37].

STEM HAADF imaging and EDX analysis were carried out along the cross section of the nanopipes. In Fig. 3, the EDX line profiles are displayed to the sides of the STEM HAADF image, showing the signals of N, Al and Ga, of the corresponding regions of interest, a cross the AlN interlayer and a cross the nanopipe (lines A and B). As expected, across the AlN interlayer (Fig. 3A), there is an increase in the Al signal and a decrease in the Ga signal, while the N signal remains constant. On the other hand, across the nanopipe (Fig.3B), the line profile does not show any significant variation between the signals of N, Al or Ga. Since no Al was detected with EDX, the change in contrast of the nanopipe observed in the HAADF image may come from variations of mass-thickness and not from element Z contrast. Contributions from strain contrast can also be ruled out, since this kind of contrast is not expected at high angles in ADF images [47]. In the case of HRTEM, a change in contrast is also observed in image of Fig. 2, but this might come from phase contrast due to variations in thickness and crystal orientation. Similar change in contrast has also been observed on inversion domains HRTEM images [48, 49], but these defects generally do not exhibit the hollow hexagonal end-on shape at the surface [48, 50, 44]. Hence, according to the dark contrast observed in the defect displayed in the HAADF STEM image and to the EDX measurements performed, we confirm that the defects observed under similar conditions correspond to nanopipes with a hollow core and not to inversion domains or nanopipes filled with GaN or AlN material.

According to F. C. Frank [51], if a dislocation has a Burgers vector that exceeds a critical value, the dislocation is then in equilibrium with an empty tube at its core. Removal of strained material and creation of internal surfaces of lower surface energy at the core become energetically favorable when strain energy associated with the dislocation is large. By balancing the surface energy created by the tube and the elastic dislocation strain energy released by the removal of material at the core, Frank showed that in an isotropic material the total energy is minimized when the empty core has a radius of

$$r = \mu b^2 / 8\pi^2 \gamma \quad (1)$$

where μ is the shear modulus, b is the magnitude of the Burgers vector and γ is the surface energy. This model fails to fit accurately for experimental observations of large diameter nanopipes with elementary screw-type Burgers vectors [32, 33], but it is useful when computing a rough estimation of the equilibrium core radius [43, 52, 53, 54]. To estimate the equilibrium radius of the hollow core nanopipe with $|\mathbf{b}| = c$ we can use equation (1) with γ=1.93 Jm^{-2} for $\{1\bar{1}00\}$ surfaces [55] and μ=122.5 GPa [56] for the GaN lattice, yielding a radius of r=0.208 nm. To estimate the hollow core equilibrium radius of the nanopipe in the AlN lattice, we can use μ=131 GPa [56] and γ=2.32 Jm^{-2} for $\{1\bar{1}00\}$ surfaces [57]. Under these considerations, equation (1) yields the equilibrium radius for the coreless dislocation in AlN as r=0.17 nm. In both materials, the equilibrium radius is rather small when $|\mathbf{b}| = c$. The cores of the nanopipes become hollow only after considering larger Burgers vectors $\mathbf{b}=n\mathbf{c}$ [53, 58]. Frank also

established a criterion for the nonlinearity case and derived an equation for a screw dislocation to become coreless after the Burgers vector exceeds a critical value:

$$b > 40\pi\,\gamma/\mu \tag{2}$$

This value is 1.98 for GaN and 2.22 for AlN, which is nearly 4 times the original value of the Burgers vector for a pure screw dislocation, **b**=4**c** (*c*=0.5178 nm in GaN and *c*= 0.4979 nm in AlN). The estimation is done considering isotropic elasticity and none of the anisotropy of the wurtzite structure. Nanopipes with big Burgers vector in GaN have been observed in confined growth structures such as nanowires [59].

As stated in equation (1), the radius of the tube, *r*, is proportional to the ratio μ/γ, and to the square of the dislocation Burgers vector, **b**. If we take the ratio r_{AlN} / r_{GaN}, assuming the same value for the Burgers vector *b*, then we can compare the μ/γ ratios of both materials and find out that the equilibrium radius for a hollow core screw dislocation in the AlN lattice is expected to be only 11% smaller than the one formed in the GaN lattice, this is $r_{AlN} = 0.89\, r_{GaN}$. This will imply that in order to keep an energy balance in the dislocation line, the nanopipe formed on the GaN lattice should reduce slightly its equilibrium radius when the dislocation continues to growth through the AlN lattice. If not, the internal surface energy of the nanopipe would no longer be in equilibrium with the dislocation line energy, and hence, the nanopipe may collapse or will start filling its core with material, yielding a full core structure.

Still, some studies suggest that the equilibrium configuration given by the Frank mechanism does not describe the formation of hollow core dislocations in GaN, and that

nanopipe formation is more in accordance to the impurity concentration and the kinetics of growth [60, 61]. Liliental-Weber et al. [16] found that Si doping was observed to reduce dislocation density but to increase nanopipes density. And in the case of GaN films with high oxygen content, the density of pinholes increased with no change in density of dislocations; similar observations were made when other dopants were present. It has been suggested that nanopipes are born at pinholes during film growth, assisted by impurity segregation which promotes and stabilizes the tubular growth of $\{1\bar{1}00\}$ facets. This is backed up by studies showing that the presence of impurities on open core screw dislocations can lower the surface energy γ of the $\{1\bar{1}00\}$ facets [62, 63]. This will of course cause an increase in the equilibrium core radius proposed in equation (1). Transformation from a normal screw dislocation into a nanopipe has also been observed to occur [64].

The termination of the nanopipe at the AlN interlayer can be influenced by the lack of impurities and by a change in the growth mode. This can be understood in the following way. During growth, the AlN interlayer is under tensile stress due to the lattice mismatch originated at the AlN/GaN interface. However, the coherent growth in the AlN interlayer is destroyed, and the structure is relaxed by the low temperature deposition of the film [37]. At this point, there is a low diffusion of impurities, which is a main factor in the growth and creation of nanopipes [61]. When lowering the deposition temperature of the AlN interlayer, the step-flow growth mode may be hindered, since it is mostly promoted by a deposition at high temperature. As a consequence, a high density of nucleation sites in the terraces is achieved by increasing the supersaturation of the growing species and by decreasing the adatoms surface mobility [36]. The transition growth mode from step flow

to nucleation on the terrace would subsequently terminate the nanopipe either by lateral overgrowth or by pinning the step edge forcing the dislocation line to bend over the GaN surface beneath the AlN layer [21]. These mechanisms are displayed in Fig. 4, where nanopipes generated at pits are terminated at the AlN interlayer. Both termination mechanisms are observed almost with the same frequency in the films, which derail us to determine if any mechanism is favored over the other.

Similar GaN films with AlN interlayers structure were tested as substrates to grow Multiple Quantum Wells (MQW) on top, and a higher carrier diffusion to the InGaN quantum wells along with a better quantum efficiency were observed [65]. Moreover, in cathodeluminescence (CL) cross section measurements, an increase of one order of magnitude was measured in GaN luminescence [66]. It would be of great interest to compare measurements of the leakage current for both structures analyzed in the present study, even though other effects have been reported to show a critical influence, such as the GaN epilayer thickness and the two dimensional electron gas (2DEG) at the AlN/GaN interface [67].

4. Conclusion

In summary, hollow nanopipes associated to screw-type threading dislocations were observed to terminate in an effective way at the AlN interlayer site in GaN films. It is proposed that the strain originated by the difference in the equilibrium core radius of the nanopipe in AlN and GaN lattices cause the nanopipes to collapse and become a screw dislocation with **b**=**c** (if the radius of the empty core is not adjusted to the equilibrium core radius). The low adatom mobility of the AlN layer during growth, may lower the

strain and the impurity segregation, promoting the termination mechanism either by hindering the step growth or by inducing lateral overgrowth of perfect material near the defect, capping the nanopipe.

Acknowledgments

The authors would like to acknowledge the technical assistance from Francisco Ruiz and Israel Gradilla and support from DGAPA-UNAM IN109612. We also thank LINAN for providing access to TEM facilities.

References

[1] A. Dadgar, Phys. Stat. Sol. B 252 (2015) 1063.

[2] F. Semond, MRS Bulletin, 40 (2015) 412.

[3] A. Dadgar, T. Hempel, J. Bläsing, O. Schulz, S. Fritze, J. Christen, and A. Krost, Phys. Stat. Sol. C 8 (2011) 1503.

[4] J. W. Chung, K. Ryu, B. Lu, and T. Palacios, Proceedings of the ESSDERC (2010) 52.

[5] Bernard Gil (Ed), III-Nitride Semiconductors and their Modern Devices, Edited by Series on Semiconductor Science and Technology 18, Oxford University Press 2013 Oxford UK 672 pages.

[6] A. Krost and A. Dadgar, Materials Science and Engineering B 93 (2002) 77.

[7] A. Dadgar, F. Schulze, J. Bläsing, A. Diez, A. Krost, M. Neuburger, E. Kohn, I. Daumiller and M. Kunze, Appl. Phys. Lett. 85 (2004) 5400.

[8] D. Zhu, D. J. Wallis and C. J. Humphreys, Rep. Prog. Phys. 76 (2013) 106501.

[9] Tingkai Li, Michael Mastro, Armin Dadgar (Eds). III–V Compound Semiconductors Integration with Silicon-Based Microelectronics CRC Press – 2010 – FL USA 603 pages.

[10] M. Cook, "GaN-on-Si opportunity for extending the life of CMOS silicon fabs?", Semiconductor Today 8 (2013) 78.

[11] F. A. Ponce, D. P. Bour, W. Götz, N. M. Johnson, H. I. Helava, I. Grzegory, J. Jun and S. Porowski, Appl. Phys. Lett. 68 (1996) 917.

[12] L. Huang, F. Liu, J. Zhu, R. Kamaladasa, E. A. Preble, T. Paskova, K. Evans, L. Porter, Y. N. Picard, R. F. Davis, J. Cryst. Growth 347 (2012) 88.

[13] F. Oehler, T. Zhu, S. Rhode, M. J. Kappers, C. J. Humphreys, R.A. Oliver, J. Cryst. Growth 383 (2013) 12.

[14] S. Nakamura and M. R. Krames, Proceedings of the IEEE 101 (2013) 2211.

[15] W. Jie-Jun, W. Kun, Y. Tong-Jun and Z. Guo-Yi, Chin. Phys. B 24 (2015) 068106.

[16] Z. Liliental-Weber, J. J. App. Phys. 53 (2014) 100205.

[17] J. W. P. Hsu, M. J. Manfra, R. J. Molnar, B. Heying, and J. S. Speck, Applied Physics Letters 81, 79 (2002).

[18] S. W. Lee, D. C. Oh, H. Goto, J. S. Ha, H. J. Lee, T. Hanada, M. W. Cho, T. Yao, S. K. Hong, H. Y. Lee, S. R. Cho, J. W. Choi, J. H. Choi, J. H. Jang, J. E. Shin, J. S. Lee, Appl. Phys. Lett. 89 (2006) 132117.

[19] M. Moseley, A. Allerman, M. Crawford, J. J. Wierer, Jr., M. Smith, and L. Biedermann, J. of Appl. Phys. 116 (2014) 053104.

[20] B. Kim, D. Moon, K. Joo, S. Oh, Y. K. Lee, Y. Park, Y. Nanishi, and E. Yoo, Appl. Phys. Lett. 104 (2014) 102101.

[21] O. Contreras, F. A. Ponce, J. Christen, A. Dadgar and A. Krost, Appl. Phys. Lett. 81, (2002) 4712.

[22] A. Dadgar, M. Poschenrieder, A. Reiher, J. Bläsing, J. Christen, A. Krtschil1, T. Finger, T. Hempel, A. Diez and A. Krost, Appl. Phys. Lett. 82, (2003) 28.

[23] F. Ruiz-Zepeda, O. Contreras, A. Dadgar, and A. Krost, Phys. Stat. Sol. C 5 (2008) 1675.

[24] A. Sagar, R. M. Feenstra1, C. K. Inoki, T. S. Kuan, Y. Fu, Y. T. Moon, F. Yun and H. Morkoç, Phys. Stat. Sol. A 202 (2005) 722.

[25] G. Cong, Y. Lu, W. Peng, X. Liu, X. Wang, Z. Wang, J. Cryst. Growth 276 (2005) 381.

[26] S. K. Mathisa, A. E. Romanov, L. F. Chen, G. E. Beltz, W. Pompe, J. S. Speck, J. Cryst. Growth 231 (2001) 371.

[27] W. Y. Fu, C. J. Humphreys, M. A. Moram, arXiv:1406.0780 (2014).

[28] S. Srinivasan, L. Geng, R. Liu, F. A. Ponce, Y. Narukawa and S. Tanaka, Appl. Phys. Lett. 83 (2003) 5187.

[29] F. A. Ponce, D. Cherns, W. T. Young and J. W. Steeds, Appl. Phys. Lett. 69 (1996) 770.

[30] D. Cherns, S. J. Henley and F. A. Ponce, Appl. Phys. Lett. 78 (2001) 2691.

[31] D. Cherns, J. Phys.: Condens. Matter 12 (2000) 10205.

[32] D. Cherns, W. T. Young, J. W. Steeds, F. A. Ponce, S. Nakamura, J. Cryst. Growth 178 (1997) 201.

[33] Z. Liliental-Weber, Y. Chen, S. Ruvimov, J. Washburn, Phys. Rev. Lett. 79 (1997) 2835.

[34] M. E. Hawkridge and D. Cherns, Appl. Phys. Lett. 87 (2005) 221903.

[35] B. Pécz, Z. Makkai, M. A. di Forte-Poisson, F. Huet, and R. E. Dunin-Borkowski Appl. Phys. Lett. 78 (2001) 1529.

[36] E. Valcheva, T. Paskova, B. Monemar, J. Cryst. Growth 255 (2003) 19.

[37] A. Dadgar, J. Bläsing, A. Diez, A. Krost, A. Alam, and M. Heuken, J. J. App. Phys. 39 (2000) L1183.

[38] J. Bläsing, A. Reiher, A. Dadgar, A. Diez, A. Krost. Appl. Phys. Lett. 81 (2002) 2722.

[39] M. Grundmann, A. Krost, D. Bimberg, Appl. Phys. Lett. 58 (1991) 284.

[40] R. Liu, F. A. Ponce, A. Dadgar, and A. Krost, Appl. Phys. Lett. 83 (2003) 860.

[41] A. Dadgar, A. Krost, J. Christen, B. Bastek, F. Bertram, A. Krtschil, T. Hempel, J. Bläsing, U. Haboeck, A. Hoffmann, J. of Cryst. Growth 297 (2006) 306.

[42] F. A. Ponce, D. Cherns, W. T. Young and J. W. Steeds, Appl. Phys. Lett. 58 (1991) 248.

[43] W. Qian, M. Skowronski, K. Doverspike, L. B. Rowland, D. K. Gaskill, J. Cryst. Growth 151 (1991) 396.

[44] P. Vennégues, B. Beaumont, M. Vaille, and P. Gibart, Appl. Phys. Lett. 70 (1997) 2434.

[45] E. Jezierska, J. L. Weyher, M. Rudzinski, and J. Borysiuk, Eur. Phys. J. Appl. Phys. 27 (2004) 255.

[46] J. L. Rouviere, M. Arlery, B. Daudin, G. Feuillet, O. Briot, Mater. Sci. and Eng. B. 50 (1997) 61.

[47] S. J. Pennycook and P. D. Nellist, Z-Contrast Scanning Transmission Electron Microscopy in: D. G. Rickerby, G. Valdrè, U. Valdrè (Eds), Impact of Electron and Scanning Probe Microscopy on Materials Research. Springer Netherlands, 1999, pp. 161-207.

[48] A. M. Sánchez, F. J. Pacheco, S. I. Molina, and R. Garcia, P. Ruterana, M. A. Sánchez-García and E. Calleja, Appl. Phys. Lett. 78 (2001) 2688.

[49] L. T. Romano, J. E. Northrup and M. A. O'Keefe, Appl. Phys. Lett. 69 (1996) 2394.

[50] L. T. Romano, B. S. Krusor, R. Singh and T. D. Moustakas, J. of Elec. Mater. 26 (1996) 285.

[51] F. C. Frank, Acta Crystallogr. 4 (1951) 497.

[52] P. Pirouz, Mat. Res. Soc. Symp. Proc. 512 (1998) 113.

[53] P. Pirouz, Phil. Mag. A, 78 (1998) 727.

[54] W. Qian, G. S. Rohrer, M. Skowronski, K. Doverspike, L. B. Rowland, and D. K. Gaskill Appl. Phys. Lett. 67 (1995) 2284.

[55] J. Northrup and J. Neugebauer, Phys. Rev. B 53 (1996) R10477.

[56] A. Polian M. Grimsditch, I. Grzegory, J. Appl. Phys. 79 (1996) 3343.

[57] S. Holec, P. H. Mayrhofer, Scripta Materialia, 67 (2012) 760.

[58] S. K. Hong, T. Yao, B. J. Kim, S. Y. Yoon, and T. I. Kim, Appl. Phys. Lett. 77 (2000) 3530.

[59] B. W. Jacobs, M. A. Crimp, K. McElroy, and V. M. Ayres, Nano Lett. 8 (2008) 4353.

[60] D. Cherns and M. E. Hawkridge, Phil. Mag. 86 (2007) 4747.

[61] D. Cherns, Microscopy and Microanalysis 12 Supp. 2 (2006) 904.

[62] J. E. Northrup, Appl. Phys. Lett. 78 (2001) 2288.

[63] J. Elsner, R. Jones, M. Haugk, R. Gutierrez, Th. Frauenheim, M. I. Heggie, S. Öberg and P. R. Briddon, Appl. Phys. Lett. 73 (1998) 3530.

[64] S. Lazar, J.LWeyher, L. Macht, F. D. Tichelaar and H. W. Zandbergen, Eur. Phys. J. Appl. Phys. 27 (2004) 275.

[65] A. Dadgar M. Poschenrieder, O. Contreras, J. Christen, K. Fehse, J. Bläsing, A. Diez, F. Schulze, T. Riemann, F. A. Ponce, and A. Krost, phys. stat. sol. (a) 192, (2002) 308.

[66] A. Dadgar, M. Poschenrieder, J. Bläsing, O. Contreras, F. Bertram, T. Riemann, A. Reiher, M. Kunze, I. Daumiller, A. Krtschil, A. Diez, A. Kaluza, A. Modlich, M. Kamp, J. Christen, F. A. Ponce, E. Kohn, A. Krost, J. of Crys. Growth 248 (2003) 556.

[67] Zhiyuan He, Yiqiang Ni, Fan Yang, Jin Wei, Yao Yao, Zhen Shen, Peng Xiang, Minggang Liu, Shuo Wang, Jincheng Zhang, Zhisheng Wu, Baijun Zhang and Yang Liu J. Phys. D: Appl. Phys.47 (2014) 045103.

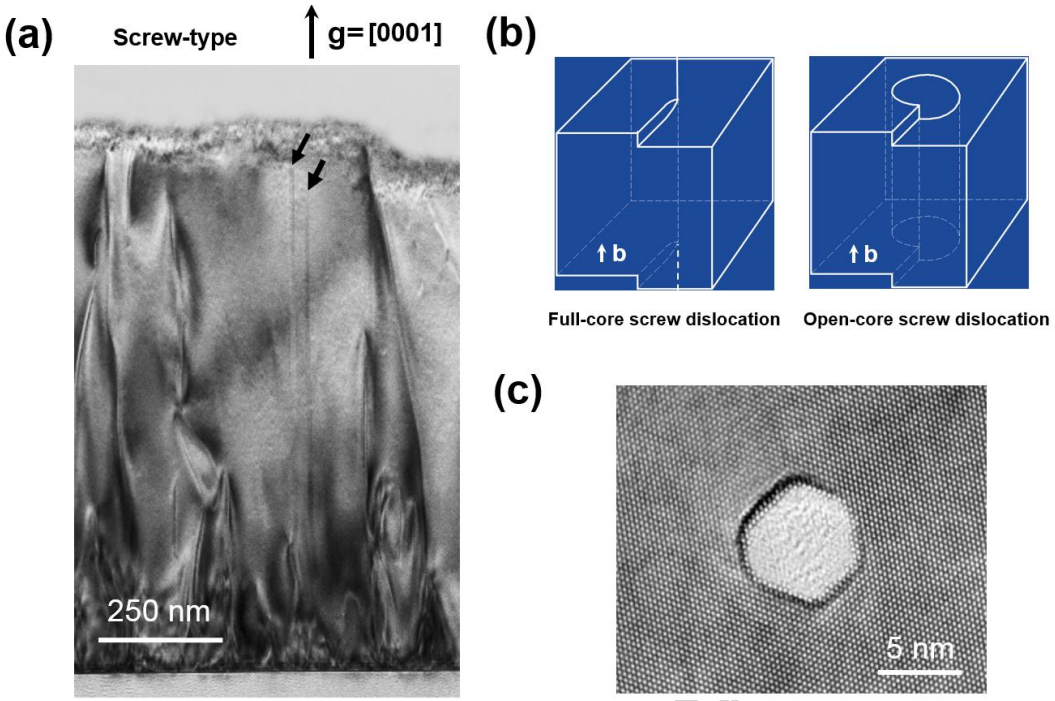

Fig. 1. (a) Cross section TEM image of GaN/Si(111) film grown with an AlN buffer layer; observed in the $[11\bar{2}0]$ zone axis and taken with **g** = [0001]. The black arrows indicate long vertical straight defects of constant width along the epilayer. (b) Full-core and open-core screw dislocation models. (c) Bright field HRTEM plan-view image of the nanopipe ending at the surface of the GaN/Si(111) heterostructure. The nanonpipe shows a hexagonal delimitation, corresponding to the $\{1\bar{1}00\}$ planes. The diameter is around 6.5 nm.

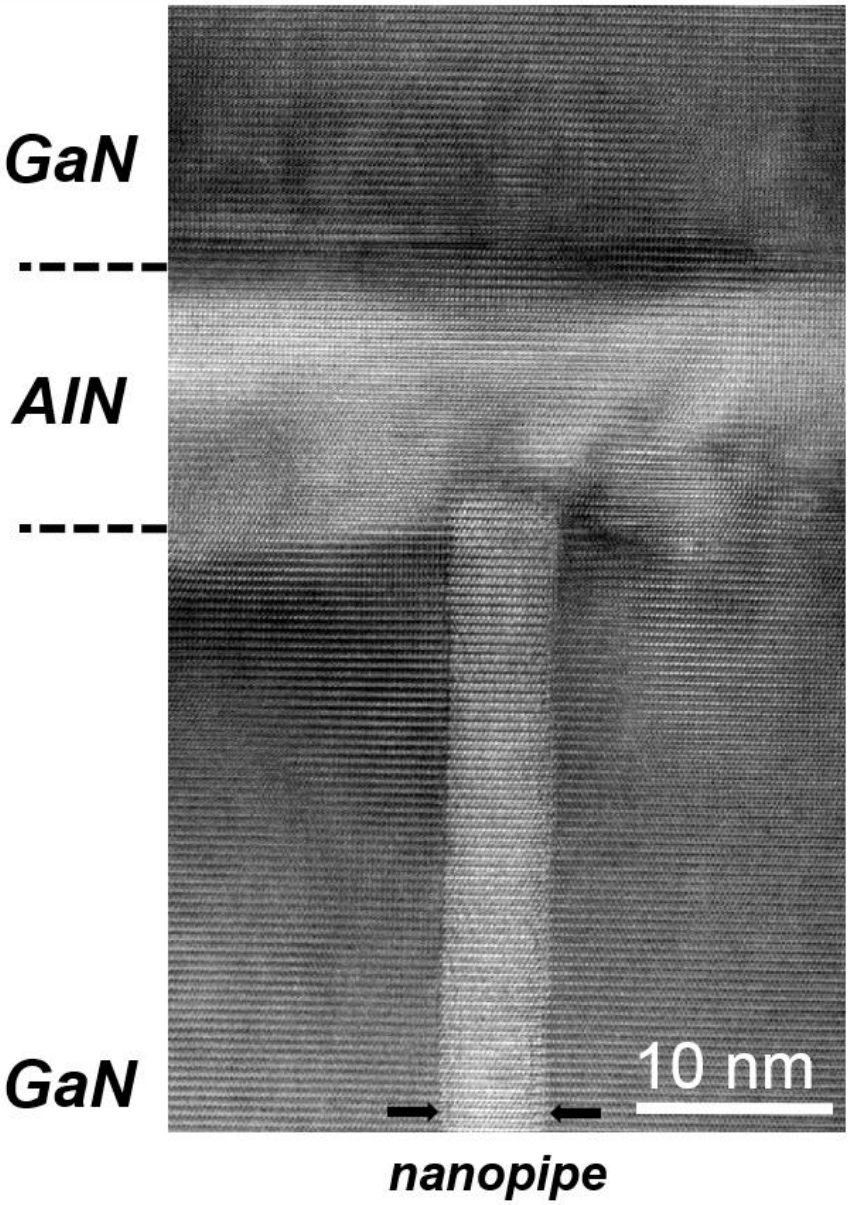

Fig. 2. Cross section HRTEM image of the nanopipe ending at the AlN interlayer, observed along $[11\bar{2}0]$ zone axis. The nanopipe shows a constant diameter of ~5.5 nm.

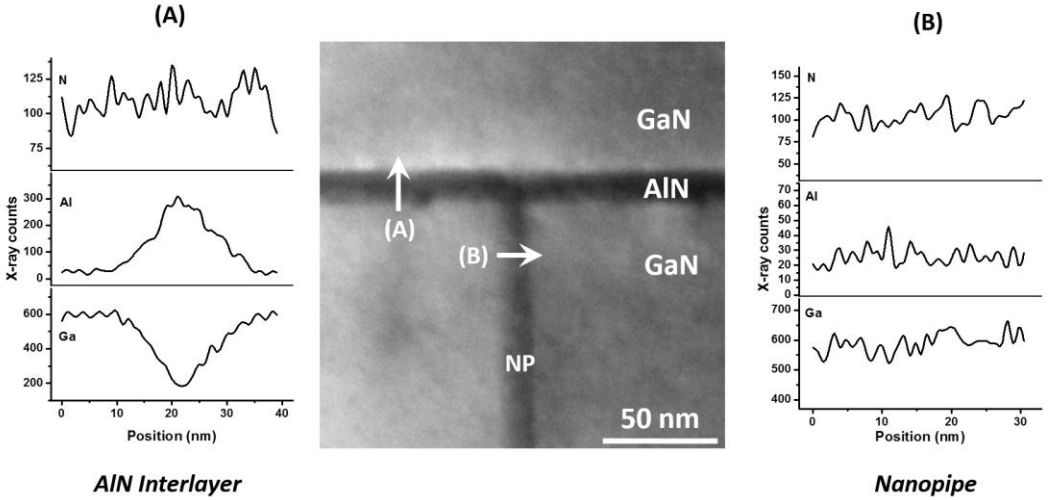

Fig. 3. STEM HAADF image and EDX line profiles of the AlN interlayer and the nanopipe (NP), shown in (A) and (B), respectively.

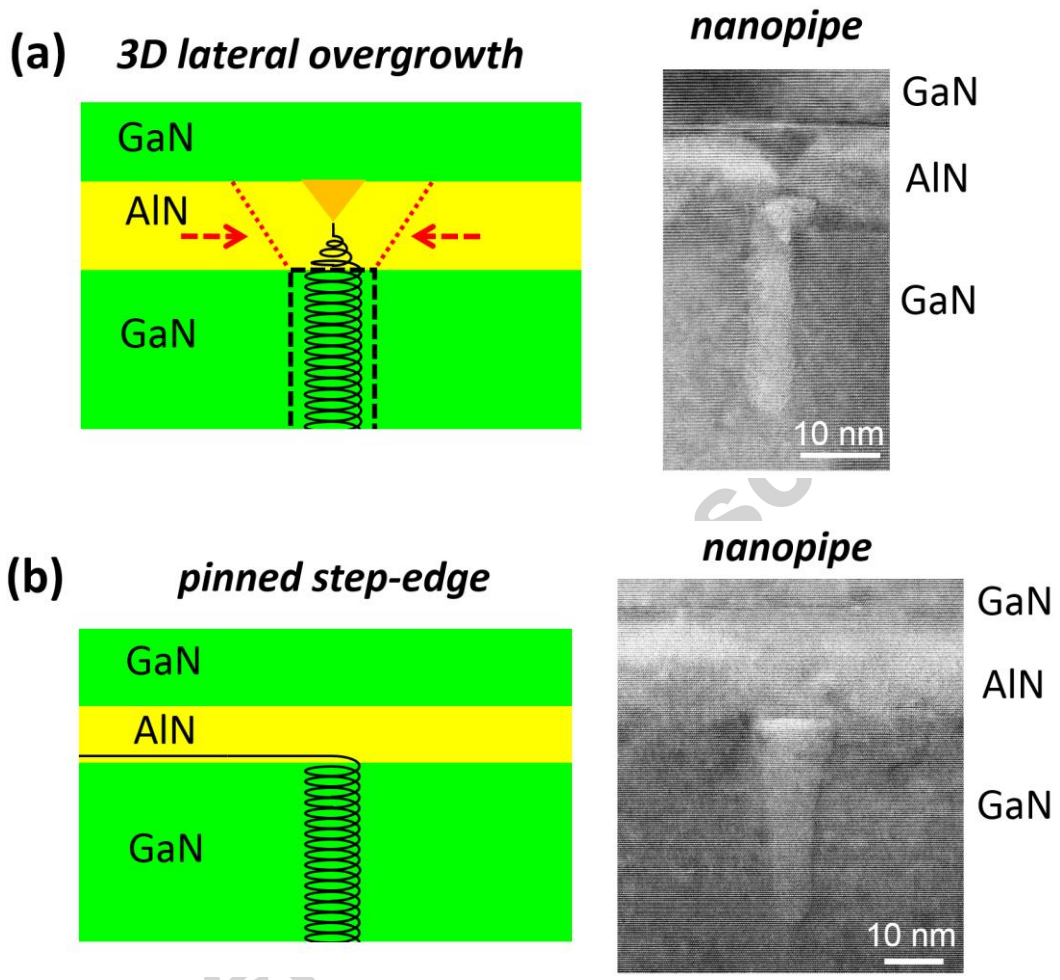

Fig. 4. Annihilation models and hollow core nanopipes observed by HRTEM at the AlN interlayer. (a) 3D lateral overgrowth and (b) pinned step-edge.

Highlights

- HRTEM and EDX are used to characterize nanopipes in GaN films grown on Si.
- AlN interlayers effectively stop the propagation of hollow core nanopipes in GaN.
- Mechanisms for the termination of nanopipes at the AlN interlayer are proposed.